Structural Eng./Earthquake Eng. Vol. 11, No. 1, 23s—31s, April 1994
Japan Society of Civil Engineers (J. Struct. Mech. Earthquake Eng. No. 489/I—27)

A PREDICTION METHOD OF ULTIMATE STRENGTH FOR STIFFENED PLATES UNDER BIAXIAL IN-PLANE FORCES

Hidenori ISAMI*

This paper presents a unified prediction method to the ultimate strength for rectangular stiffened plates under biaxial in-plane forces in the elasto-plastic range. For a given strain ratio in two biaxial directions, the elasto-plastic buckling strength is obtained from the elasto-plastic material behavior and the residual stresses in two directions. Then the elasto-plastic ultimate strength is predicted in terms of the imperfection sensitivity curve in the neighborhood of the particular point, where the elasto-plastic post-buckling curve intersects the pathological failure mechanism curve. The ultimate strength is found to be in good agreement with the previous numerical results.

Key Words : *Ultimate strength, Stiffened plates, Biaxial in-plane forces, Nonlinear bifurcation theory, Imperfection-sensitivity*

1. INTRODUCTION

Thin plates used as members of flange plates of box girders and chords of trusses and arches, bridge piers and towers are subjected to compression, tension, bending, shear and their complicated combinations. Especially, the stability and strength of stiffened plates under biaxial in-plane forces have been the subjects of the greatest concern of civil engineers. However, there has been only a little investigation on the ultimate behavior and strength of stiffened plates in the biaxial case, comparing with researches in the uniaxial case.[1),2),3)]

Prabhakara *et al.*[4)], Libove[5)], Haslach[6)] and Zhang *et al.*[7)] examined the elastic buckling and the postbuckling properties of biaxially compressed orthotropic plates using the well-known fundamental equilibrium differential equation. Also, Ueda *et al.*[8)] proposed a new elastic buckling interaction equation for rectangular plates under combinations of compression, bending and shear.

Valsgård[9)] proposed a conservative interaction formula of biaxially compressed plates from numerical results of nonlinear shell analysis. Dowling *et al.*[10)] examined the ultimate strength of rectangular plates under biaxial forces by the finite difference procedure using dynamic relaxation. They made several parametric studies in order to clarify the effects of aspect ratio, slenderness and initial imperfection such as geometric deformations and residual stresses on the ultimate strength. Also, Narayanan *et al.*[11)] presented an approximate prediction of the post-buckling and collapse behavior for biaxially compressed plates using their energy method.

In Japan, Inoue *et al.*[12)] evaluated the buckling stress and strain of biaxially compressed plates in the elastic, plastic flow and strain-hardening range using explicit formulations of the out-of-plane flexural rigidities at an instance of buckling. Ohtsubo *et al.*[13)] proposed a simplified interaction curve of ultimate strength of biaxially compressed plates, based on the results by the finite element nonlinear analysis. Also, a design curve of the ultimate strength of a single panel under biaxial compression is presented from the experimental results by Mikami *et al.*[14)]

Furthermore, Kitada *et al.*[15),16)] developed a design method of stiffened plates under uniaxial and biaxial in-plane forces, and proposed interaction curves accurately approximating their numerical results. Also, Kumagai *et al.*[17)] proposed a simple equation of prediction on the required flexural rigidities of stiffeners of biaxially loaded stiffened plates.

These analytical and numerical methods allow the maximum ultimate strength of biaxially forced plate members to be determined in an isolated form for a selected set of several geometrical and material parameters.

The author has proposed a unified method to predict the ultimate strength of slender steel structures such as compressed columns, uniaxially compressed plates with or without stiffeners, compressed cylindrical shells, compressed cylindrical panels and biaxially compressed plates with or without stiffeners in the elasto-plastic range.[18),19),20),21)]

This paper will present a prediction method of the elasto-plastic ultimate strength for simply supported rectangular plates with longitudinal stiffeners under biaxial in-plane forces of tension and/or compression. This method will develop the approach in the author's previous researches.[19),21)] Some numerical

* Member of JSCE, Dr.Eng., Department of Civil Engineering, Kochi National College of Technology (200-1, Monobe-Otsu, Nankoku, Kochi, Japan 783)

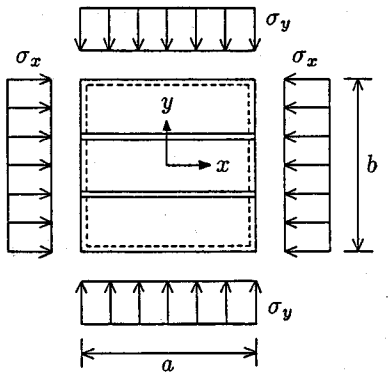

Fig. 1-a Biaxially forced stiffened plates.

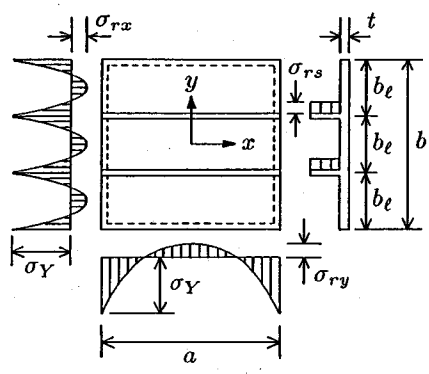

Fig. 1-b Residual stress distributions.

Fig. 1 Stiffened plates under biaxial in-plane forces ($n_S = 2$).

demonstrations will clarify the validity and applicability of the proposed method.

2. BASIC FORMULATIONS

(1) Assumptions.

A simply supported, rectangular steel stiffened plate with n_S longitudinal stiffeners under biaxial in-plane forces σ_x and σ_y is analyzed using a typical basic model shown in **Fig. 1-a**. The torsional rigidity of a stiffener is neglected in this analysis. The material behaves to be elastic and perfectly plastic. All the stresses are non-dimensionalized by the material yielding stress σ_Y. Also, the stress is taken positive when it produces compression.

A stiffener has the following parameters:

$$\delta = \frac{A_S}{bt} \quad \text{and} \quad \gamma = \frac{EI_S}{bD_e} \qquad \cdots\cdots (1)$$

where δ and γ refer to the ratio of the cross-sectional area of a stiffener and the ratio of its flexural rigidity to that of the global plate panel, respectively. Herein, E is the Young's modulus being the constant in both materials of the plate panel and of the stiffener. Moreover, t and b indicate the thickness and the width of the global plate panel, and $D_e = Et^3/[12(1-\nu^2)]$ and ν are the flexural rigidity of the panel and Poisson's ratio of the material. A_S and I_S refer to the cross-sectional area and the moment of inertia of a stiffener.

As shown in **Fig. 1-b**, each residual stress in the cross section perpendicular to the longitudinal x- or the transverse y-direction is assumed to be distributed symmetrically with respect to the x- or y-axis in the n_x- or n_y-th order curve of the coordinate x or y, respectively. σ_{rx} and σ_{ry} refer to the magnitudes of the non-dimensionalized maximum compressive residual stresses in x- and y-directions, respectively.

A stiffener is assumed to have a uniform distribution of tensile residual stress with its non-dimensionalized magnitude σ_{rs} in the cross section. Such distributions of residual stresses seem to interpolate those in some previous numerical analyses.[10),15),16)] Then, the non-dimensionalized average axial stress σ_x or σ_y and the average strain ε_x or ε_y can be defined independently in the x- or y-direction:[21)]

$$\begin{cases} \sigma_i &= 1 + \kappa_i(1+\sigma_{ri})(1-\kappa_i)^{n_i} \\ &\quad - \dfrac{1+\sigma_{ri}}{n_i+1}\left[\,1-(1-\kappa_i)^{n_i+1}\,\right] \\ \varepsilon_i &= \dfrac{\sigma_Y}{E}\left[\,1+(1+\sigma_{ri})(1-\kappa_i)^{n_i}-\sigma'_{ri}\,\right] \\ &\qquad (i = x \text{ or } y) \end{cases} \qquad (2)$$

for an in-plane compression, and

$$\begin{cases} \sigma_i &= -1 + \dfrac{n_i}{n_i+1}(1+\sigma_{ri})\kappa_i^{n_i+1} \\ \varepsilon_i &= \dfrac{\sigma_Y}{E}\left[\,-1+(1+\sigma_{ri})\kappa_i^{n_i}-\sigma'_{ri}\,\right] \\ &\qquad (i = x \text{ or } y) \end{cases} \qquad \cdots\cdots (3)$$

for an in-plane tension, in which

$$\begin{cases} \sigma'_{rx} &= \sigma_{rx} - \overline{\sigma}_{rs}\,, \quad \sigma'_{ry} = \sigma_{ry} \\ n_x &= \dfrac{1+\overline{\sigma}_{rs}}{\sigma_{rx}-\overline{\sigma}_{rs}}\,, \quad n_y = \dfrac{1}{\sigma_{ry}} \\ \overline{\sigma}_{rs} &= \dfrac{n_S\delta}{1+n_S\delta}\sigma_{rs} \end{cases} \qquad \cdots\cdots (4)$$

and κ_x or κ_y denotes the ratio of the elastic portion of the cross section to the total cross section perpendicular to x- or y-direction, respectively.

Thus, the tangent modulus E_{tx} or E_{ty} can be defined independently in each direction using the ratio κ_x or κ_y:

$$E_{ti} = \frac{d\sigma_i}{d\varepsilon_i} = \kappa_i E \qquad (i = x \text{ or } y) \qquad \cdots\cdots (5)$$

Furthermore, the global secant modulus E_S of the stiffened plate can be obtained as follows:

$$E_S = \frac{\sigma_{eq}}{\varepsilon_{eq}} \frac{\sigma_Y}{E} E \quad \cdots\cdots (6)$$

where σ_{eq} denotes the non-dimensionalized equivalent stress, and ε_{eq} is the corresponding equivalent strain:

$$\begin{cases} \sigma_{eq} &= \sqrt{\sigma_x^2 + \sigma_y^2 - \sigma_x \sigma_y} \\ \varepsilon_{eq} &= \sqrt{\varepsilon_x^2 + \varepsilon_y^2 - \varepsilon_x \varepsilon_y} \end{cases} \quad \cdots\cdots (7)$$

(2) Elasto-plastic buckling strength

Assuming all edges of this stiffened plate model in **Fig. 1** to be simply supported, the buckling mode and the initial geometric imperfection mode are

$$\begin{cases} W &= w \cos\frac{m\pi x}{a} \cos\frac{n\pi y}{b} \\ W_o &= w_o \cos\frac{m\pi x}{a} \cos\frac{n\pi y}{b} \end{cases} \quad \cdots\cdots (8)$$

where W and W_o designate the out-of-plane deflection and the initial out-of-plane deflection, and w and w_o refer to the magnitudes of the buckling mode and the initial deflection mode, respectively, with m- and n-half wave numbers in the longitudinal and transverse directions. All out-of-plane deflections and modes are non-dimensionalized by the thickness t of the plate panel.

Using the secant modulus E_S in Eq. (6) and the modified Airy's stress function F, the nonlinear fundamental equations of equilibrium of the orthotropic 'perfect' plate with no initial deflections ($W_o = 0$) in the elasto-plastic range can be written as:

$$\begin{cases} \nabla^4 \tilde{F} &= \frac{E_S}{E} \frac{E}{\sigma_Y} \{(W_{,xy})^2 - W_{,xx} W_{,yy}\} \\ \nabla_p^4 W &= \frac{1}{D_p} \{ t_x \tilde{F}_{,yy} W_{,xx} + \tilde{F}_{,xx} W_{,yy} \\ & \qquad - 2\tilde{F}_{,xy} W_{,xy} \} \end{cases} \quad (9)$$

where

$$\begin{cases} \nabla^4 \tilde{F} &= \tilde{F}_{,xxxx} + 2\tilde{F}_{,xxyy} + \tilde{F}_{,yyyy} \\ \nabla_p^4 W &= k_1 W_{,xxxx} + 2(k_2 + 2k_4) W_{,xxyy} \\ & \qquad + k_3 W_{,yyyy} \end{cases} \quad \cdots (10)$$

and

$$\begin{cases} \tilde{F} &= \frac{F}{\sigma_Y t^2}, \quad D_p = \frac{D_e}{\sigma_Y t^3} \\ t_x &= 1 + (n_S + 1)\delta \end{cases} \quad \cdots\cdots (11)$$

Furthermore, t_x and k_j (j =1,2,3 and 4) show the non-dimensionalized equivalent thickness ratio of the orthotropic plate to the panel thickness t and some constants to designate flexural and torsional rigidities of the orthotropic plate in the elasto-plastic range. Here, the subscripts behind the comma of W or $\tilde{F}$ mean taking derivatives with respect to coordinates of x and y.

Expanding the Bleich's approach[22], these coefficients k_j are defined in the elasto-plastic range as follows:

$$\begin{cases} k_1 &= \kappa_x \{ 1 + (n_S + 1)\gamma \} \\ k_2 &= \sqrt{\kappa_x}\sqrt{\kappa_y} \\ k_3 &= \kappa_y \quad \text{and} \quad k_4 = \frac{1-\nu}{2}\sqrt{\kappa_x}\sqrt{\kappa_y} \end{cases} \quad \cdots\cdots (12)$$

where κ_x and κ_y can be evaluated from Eq. (5) using Eq. (2) or Eq. (3).

Substituting E_S of Eq. (6), W of Eq. (8) and coefficients k_j of Eq. (12) into Eqs. (9), (10) and (11), and using the Galerkin's method, the post-buckling equilibrium path σ_{eq} of the 'perfect' plate in the elasto-plastic range can be obtained using the critical buckling stress σ_{eq}^p in the parabolic form of the buckling mode w:

$$\sigma_{eq} = \sigma_{eq}^p + C_p w^2 \quad \cdots\cdots (13)$$

where (i)σ_x-buckling, when the buckling is considered to occur mainly in the longitudinal direction, including the longitudinal uniaxial case of $\sigma_y = 0$ for the stress ratio $\rho = \sigma_y/\sigma_x = 0$:

$$\begin{cases} \sigma_{eq} &= \sigma_x \sqrt{1 - \rho + \rho^2} \\ \sigma_{eq}^p &= \sigma_x^p \sqrt{1 - \rho + \rho^2} \\ C_p &= C_{px} \sqrt{1 - \rho + \rho^2} \end{cases} \quad \cdots\cdots (14)$$

and

$$\begin{cases} \sigma_x^p &= f_x^p \sigma_x^e, \quad \sigma_x^e = \frac{1}{R_x^2} \\ R_x &= \frac{b}{t}\sqrt{\frac{12(1-\nu^2)}{\pi^2 K_x}\frac{\sigma_Y}{E}} \\ K_x &= \frac{C_{\alpha\phi}}{t_{\alpha\phi}^x}, \quad K_y = \rho K_x \\ f_x^p &= \frac{C_{\alpha\phi}^p}{C_{\alpha\phi}}, \quad C_{px} = \frac{C_x C'_{\alpha\phi}}{t_{\alpha\phi}^x} \end{cases} \quad \cdots\cdots (15)$$

(ii)σ_y-buckling, when the buckling is considered to occur mainly in the transverse direction, including the transverse uniaxial case of $\sigma_x = 0$ for $\rho \to \infty$:

$$\begin{cases} \sigma_{eq} &= \sigma_y \sqrt{1 - \rho + \rho^2} \,/\, \rho \\ \sigma_{eq}^p &= \sigma_y^p \sqrt{1 - \rho + \rho^2} \,/\, \rho \\ C_p &= C_{py} \sqrt{1 - \rho + \rho^2} \,/\, \rho \end{cases} \quad \cdots\cdots (16)$$

and

$$\begin{cases} \sigma_y^p &= f_y^p \sigma_y^e, \quad \sigma_y^e = \frac{1}{R_y^2} \\ R_y &= \frac{b}{t}\sqrt{\frac{12(1-\nu^2)}{\pi^2 K_y}\frac{\sigma_Y}{E}} \\ K_y &= \frac{C_{\alpha\phi}}{t_{\alpha\phi}^y}, \quad K_x = K_y/\rho \\ f_y^p &= \frac{C_{\alpha\phi}^p}{C_{\alpha\phi}}, \quad C_{py} = \frac{C_y C'_{\alpha\phi}}{t_{\alpha\phi}^y} \end{cases} \quad \cdots\cdots (17)$$

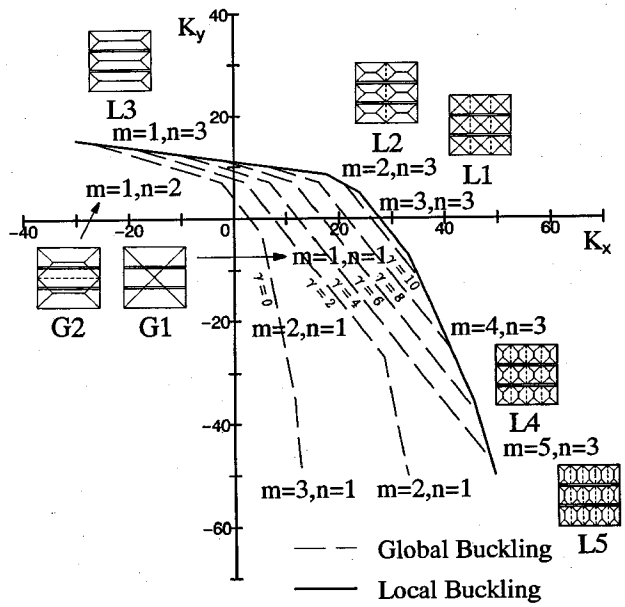

Fig. 2 Interaction curves of elastic buckling coefficients ($n_S = 2, \phi = 1, \delta = 0.1$).

in which,

$$C^p_{\alpha\phi} = \frac{\{\sqrt{\kappa_x}(\frac{\alpha}{\phi}) + \sqrt{\kappa_y}(\frac{\phi}{\alpha})\}^2 + \kappa_x(n_S+1)\gamma\,(\frac{\alpha}{\phi})^2}{(\frac{\alpha}{\phi} + \frac{\phi}{\alpha})^2 + (n_S+1)\gamma\,(\frac{\alpha}{\phi})^2}$$

$$C_{\alpha\phi} = n^2\{(\frac{\alpha}{\phi} + \frac{\phi}{\alpha})^2 + (n_S+1)\gamma\,(\frac{\alpha}{\phi})^2\}$$

$$C'_{\alpha\phi} = n^2\{(\frac{\alpha}{\phi})^2 + (\frac{\phi}{\alpha})^2\} \quad \cdots\cdots (18)$$

$$t^x_{\alpha\phi} = 1 + (n_S+1)\delta + \rho\,(\frac{\phi}{\alpha})^2$$

$$t^y_{\alpha\phi} = \frac{1 + (n_S+1)\delta}{\rho} + (\frac{\phi}{\alpha})^2$$

$$C_x = \frac{3(1-\nu^2)}{4K_x}\,\frac{1}{R_x^2}\,\frac{E_S}{E}$$

$$C_y = \frac{3(1-\nu^2)}{4K_y}\,\frac{1}{R_y^2}\,\frac{E_S}{E}$$

and, at the instance of buckling, the stress ratio $\rho = \sigma_y/\sigma_x$ is evaluated from Eq. (2) or Eq. (3) if the strain ratio $\rho' = \varepsilon_y/\varepsilon_x$ is specified at the critical buckling point, and the same value of ρ is used in the post-buckling range. Also, $\alpha = m/n$ is the ratio of the longitudinal wave-number m to the transverse wave-number n of buckling mode concerned, and $\phi = a/b$ is the aspect ratio of the global stiffened plate. Moreover, R_x, K_x and σ^e_x refer to the generalized width-thickness ratio of the plate, the elastic buckling coefficient and the non-dimensionalized Euler buckling stress, respectively, in the longitudinal x-direction. Similarly, R_y, K_y and σ^e_y refer to those in the transverse y-direction.

In Eq. (15) or Eq. (17), if $\delta = 0$ and $\gamma = 0$, then some parameters are entirely the same that those for unstiffened plate subjected to biaxial in-plane forces, expanding the author's previous methods.[18),19)] Also, elastic buckling coefficients K_x and K_y for stiffened plates are equivalent to those proposed by Kitada *et al.*[16)]

(3) Minimum flexural rigidity

In the elastic range, the strain ratio ρ' always equals to the corresponding stress ratio $\rho = K_y/K_x$. Hence, eliminating ρ in Eq. (15) or Eq. (17), an interaction curve of elastic buckling coefficients for global buckling of the stiffened plate leads to the following straight line:

$$K_x + C_1 K_y = C_2 \quad \cdots\cdots (19)$$

where

$$C_1 = \frac{t_{\alpha\phi}}{t_x}\,,\ C_2 = \frac{C_{\alpha\phi}}{t_x} \ \text{and} \ t_{\alpha\phi} = (\frac{\phi}{\alpha})^2 \quad \cdots\cdots (20)$$

Also, an interaction curve for local buckling of the plate panel is expressed in the form of the similar straight line:

$$K_x + C^\ell_1 K_y = C^\ell_2 \quad \cdots\cdots (21)$$

where C^ℓ_1 and C^ℓ_2 are obtained from C_1 and C_2, respectively, in Eq. (20) when $\delta = 0$ and $\gamma = 0$.

Fig. 2 shows the interaction curve of elastic buckling coefficients when $n_S = 2$, $\phi = 1$ and $\delta = 0.1$. Solid lines indicate the interaction curves for local buckling of the plate panel, and are composed of five straight lines corresponding to five buckling modes of L3;$\alpha_\ell = 1/3\,(m = 1, n = 3)$, L2;$\alpha_\ell = 2/3\,(m = 2, n = 3)$, L1;$\alpha_\ell = 1\,(m = 3, n = 3)$, L4;$\alpha_\ell =$

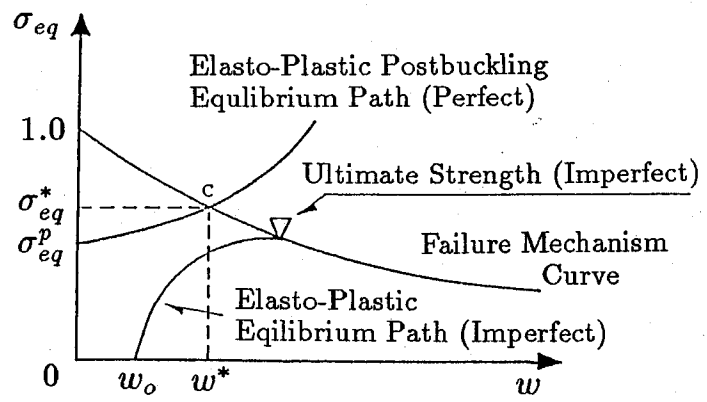

Fig. 3 Equivalent bifurcation point and ultimate strength.

$4/3\,(m=4,n=3)$ and L5;$\alpha_\ell = 5/3\,(m=5,n=3)$. Moreover, dashed lines indicate the interaction curves for global buckling of the stiffened plate when the flexural rigidity γ ranges 0 to 10, and each curve is composed of four straight lines corresponding to four buckling modes of G2;$\alpha = 1/2\,(m=1,n=2)$, G1;$\alpha = 1\,(m=1,n=1)$, G3;$\alpha = 2\,(m=2,n=1)$ and G4;$\alpha = 3\,(m=3,n=1)$. Herein, as found in **Fig. 2**, two global modes of G1 and G2 are only considered because the other two modes of G3 and G4 little affect the prediction of the ultimate strength. Therefore, seven failure mechanisms corresponding to seven buckling modes of L1, L2, L3, L4, L5, G1 and G2 are illustrated in this figure.

Now, if ρ, ϕ, α, α_ℓ, n_S and δ are given, then the minimum flexural rigidity γ^* of a stiffener can be obtained from coincidence of both types of buckling coefficients for global stiffened plate and local plate panel in Eq. (19) and Eq. (21).

$$\gamma^* = \frac{\dfrac{C_2^\ell\{1+(n_s+1)\delta+\rho(\frac{\phi}{\alpha})^2\}}{(1+C_1^\ell\rho)n^2} - (\frac{\alpha}{\phi}+\frac{\phi}{\alpha})^2}{(n_s+1)(\frac{\alpha}{\phi})^2} \quad \cdots\cdots (22)$$

Fig. 2 shows that an intersection point of a solid line and a dashed line specifies an appropriate value of the stress ratio $\rho = K_y/K_x$ when $\gamma = \gamma^*$. In order to compare the present results with those by Kitada *et al.*[16], several explicit relationships between γ^* and ρ are defined from Eq. (22) for σ_x- and/or σ_y-buckling.[21]

(4) Failure mechanism

Ultimate strength of stiffened plates can not be generally determined by evaluating the elasto-plastic critical buckling strength and the post-buckling path from the residual stress. It is further affected by the initial out-of-plane deflection and the plastic unloading curve forming the failure mechanism.

Herein, the following interaction formula between the non-dimensionalized equivalent stress σ_{eq} in Eq. (7) and the non-dimensionalized bending moment m_p on fold lines of each failure mechanism is assumed for simplicity:[23]

$$\sigma_{eq}^2 + m_p^2 = 1 \quad \cdots\cdots (23)$$

where $m_p = M/M_p$; M and M_p refer to the bending moment perpendicular to the plastic fold line and the full plastic moment, respectively. Each failure mechanism has the plastic fold line designated as the solid line, as shown in **Fig. 2**.

The failure mechanism curves for G1 and G2 can be expressed in the following form:[20),21),23]

$$w = A_p \frac{\sqrt{1-\sigma_{eq}^2}}{\sigma_{eq}} \quad \cdots\cdots (24)$$

where

$$A_p = \begin{cases} \dfrac{1+\delta(h_S/t)}{1+\rho+(4/3)\delta}\sqrt{1-\rho+\rho^2} & \text{for G1} \\ \dfrac{3+2\delta(h_S/t)}{2\{1+3\rho+(8/3)\delta\}}\sqrt{1-\rho+\rho^2} & \text{for G2} \end{cases} \quad (25)$$

which h_S is the height of a stiffener. Hence, h_S/t can be defined from several parameters as above mentioned.

Furthermore, values of A_p in Eq. (24) for failure mechanisms of L1, L2, L3, L4, and L5 are similarly obtained from modifying those for biaxially compressed unstiffened plates.[18),19]

(5) Ultimate strength

Now, define an 'equivalent bifurcation point' as the intersection of the elasto-plastic post-buckling path of Eq. (13) with the failure mechanism curve of Eq. (24). The point can be obtained by solving the following cubic polynomial equation:[18),19),20),21]

$$\sigma_{eq}^3 - (\sigma_{eq}^p - C_p A_p^2)\,\sigma_{eq}^2 - C_p A_p^2 = 0 \quad \cdots\cdots (26)$$

Let σ_{eq}^* and w^* designate a proper real root of the equation and the corresponding deflection calculated

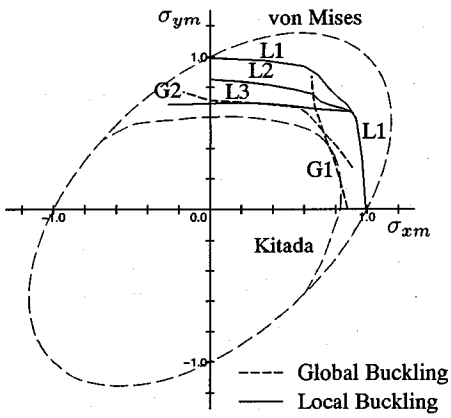

Fig. 4 Interaction curves for square stiffened plates ($b_\ell/t = 30, W_o t = a/1000$).

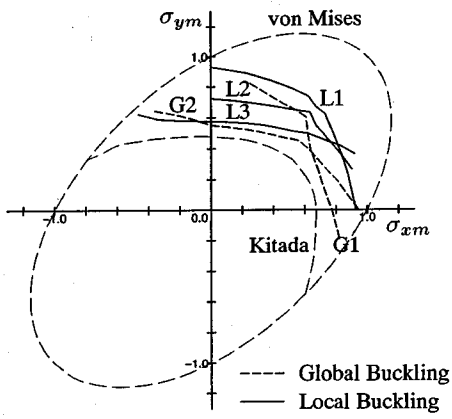

Fig. 5 Interaction curves for square stiffened plates ($b_\ell/t = 40, W_o t = a/1000$).

from Eq. (24). Then, the point $C(w^*, \sigma^*_{eq})$ in **Fig. 3** gives the 'equivalent bifurcation point' of the 'perfect' plate.

In order to evaluate the ultimate strength of the 'imperfect' plate with the initial deflection mode w_o, a pseudo-potential may be defined near the equivalent bifurcation point C. The non-dimensionalized equivalent ultimate strength σ_m can be predicted to have the maximum value on the failure mechanism curve. Then, σ_m is expressed in terms of the following unified form through the nonlinear bifurcation theory.[18),19),20),21)]

$$\sigma_m = \sigma^*_{eq}[1 + \alpha^* w^*_o - \sqrt{2\alpha^* w^*_o(1 + \frac{1}{2}\alpha^* w^*_o)}\,] \quad \cdots (27)$$

where α^* can be obtained by the slope of the failure mechanism curve, Eq. (24), at the equivalent bifurcation point C:

$$\alpha^* = -\frac{1}{\sigma^*_{eq}}\frac{d\sigma_{eq}}{dw}\Big|_{\sigma_{eq}=\sigma^*_{eq}} = \frac{\sigma^*_{eq}\sqrt{1-\sigma^{*2}_{eq}}}{A_p} \quad \cdots (28)$$

and w^*_o is an 'equivalent initial deflection mode' defined by

$$w^*_o = \mu(R) w_o \quad \cdots (29)$$

Moreover, R refers to the generalized width-thickness ratio, being R_x in Eq. (15) or R_y in Eq. (17). Also, R_p is a particular value of R, at which the critical buckling point changes from the elasto-plastic to purely elastic.

An explicit expression of $\mu(R)$ is determined taking into reasonable account the consistency and unification with strength prediction formulas for other structural elements such as beams, columns, plates and shells,[18),19),20),21)] as well as comparing with a few numerical researches:[10),11),15),16)]

$$\mu(R) = \mu_c(\frac{R}{R_p})^\beta\ ,\ \beta = 2(1 - \frac{R}{R_p})\ ,\ \mu_c = \frac{1}{4} \quad \cdot (30)$$

Finally, the ultimate strengths σ_{xm} and σ_{ym} in the longitudinal and transverse directions can be calculated from taking $\sigma_{eq} = \sigma_m$ in Eq. (7) through Eq. (27). Thus,

$$\sigma_{xm} = \frac{\sigma_m}{\sqrt{1-\rho+\rho^2}} \quad \text{and} \quad \sigma_{ym} = \rho\,\sigma_{xm} \quad \cdots\cdots (31)$$

for the specified value of the stress ratio ρ.

3. NUMERICAL DEMONSTRATIONS AND DISCUSSIONS

Now, let us examine square stiffened plates with two longitudinal stiffeners under biaxial in-plane forces, and compare these ultimate strengths with the numerical results by Kitada *et al.*[16)] Stiffened plates considered have $\phi = 1$, $n_S = 2$, $\delta = 0.1$ and $\gamma = \gamma^*$, and the material is always $\sigma_Y/E = 1/875$. The magnitudes of the maximum compressive residual stresses in the local plate panel and of the constant tensile residual stress in a stiffener are assumed to be $\sigma_{rx} = \sigma_{ry} = 0.3$ and $\sigma_{rs} = 0.2$, respectively. Moreover, two types of global and local initial deflections are independently specified as $a/1000$ and $b_\ell/150$ ($b_\ell = b/3$). Two types of global buckling modes of G1 and G2, and five types of local panel buckling modes of L1, L2, L3, L4, and L5 are taken into account herein.

Figs. 4, 5 and **6** show the interaction curves of square stiffened plates for the width-thickness ratio b_ℓ/t=30, 40 and 60, respectively. The abscissa indicates the longitudinal ultimate strength σ_{xm} and the ordinate indicates the transverse ultimate strength σ_{ym}, where both can be predicted by Eq. (31) through Eq. (27). The global initial deflection is assumed to be $a/1000$. Herein, the solid lines indicate the ultimate strengths for local panel

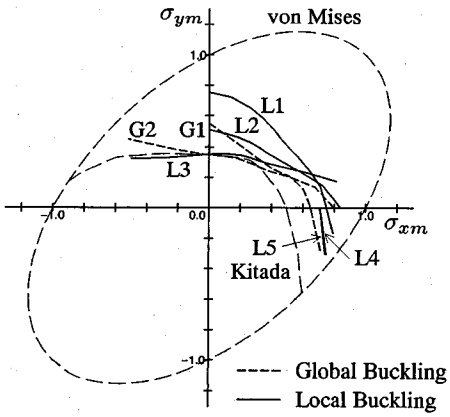

Fig. 6 Interaction curves for square stiffened plates ($b_\ell/t = 60, W_o t = a/1000$).

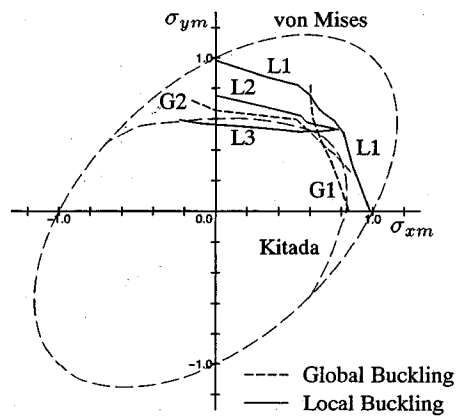

Fig. 7 Interaction curves for square stiffened plates ($b_\ell/t = 30, W_o t = b_\ell/150$).

buckling modes of L1, L2 , L3, L4 and L5, and the regular dashed lines indicate the ultimate strengths for global buckling modes of G1 and G2. Also, the long dashed lines are the von Mises's yield condition and the ultimate strength by Kitada *et al.*[16]

Therefore, the present ultimate strength can be conservatively predicted by an envelope curve of seven interaction curves for seven types of failure mechanisms corresponding to seven buckling modes.

For the elasto-plastic buckling of stocky stiffened plates with smaller width-thickness ratio $b_\ell/t = 30$ in **Fig. 4**, it is found that the ultimate strength obtained from buckling modes of G1, G2 and L3 is more unsafe than the Kitada's numerical results.

The interaction curves for intermediate practical width-thickness ratio $b_\ell/t = 40$ in **Fig. 5** are shown to be slightly more unsafe than those by Kitada for G1, G2 and L3, like **Fig. 4**.

Also, for the elastic buckling of relatively slender stiffened plates with larger width-thickness ratio b_ℓ/t=60 in **Fig. 6**, the ultimate strength for G2 and L3 is almost in good agreement with those by Kitada, and is slightly more unsafe than those for G1.

Figs. 7, 8 and **9** show the interaction curves of square stiffened plates with local initial deflection of $b_\ell/150$ for the width-thickness ratio b_ℓ/t=30, 40 and 60, respectively. Similarly, seven interaction curves corresponding to seven types of buckling modes are presented herein.

For the elasto-plastic buckling of stocky stiffened plates with smaller width-thickness ratios of $b_\ell/t = 30$ and $b_\ell/40$ in **Fig. 7** and **Fig. 8**, it is also found that the ultimate strength for G1, G2 and L3 is conservatively in good agreement with the Kitada's results. Naturally in the case of pure longitudinal or transverse buckling, the present strength approximates the Kitada's result very well. Thus, the present method provides the proper ultimate strength for these practical ranges of width-thickness ratios.

Moreover, for the elastic buckling for larger width-thickness ratio b_ℓ/t=60 in **Fig. 9**, the ultimate strength in $\sigma_{xm} < \sigma_{ym}$ is slightly more conservative than those by Kitada, while the former in $\sigma_{xm} > \sigma_{ym}$ is slightly more unsafe than the latter.

The present analysis is seemed to evaluate the accurate ultimate strength for pure transverse buckling, and however, to slightly overestimate the ultimate strength for pure longitudinal buckling, comparing with the Kitada's results. This overestimation tends to become lighter for smaller width-thickess ratio.

The author proposed the similar approach to the ultimate strength of unstiffened plates under biaxial compression,[18),19)] and found that his results are in good agreement with those by Dowling[10)] and Kitada *et al.*[15),16)] Thus, the ultimate strength for local buckling of the plate panel of the stiffened plate may be evaluated with wonderful accuracy.

The ultimate strength of stiffened plates with the flexural rigidity of $\gamma = \gamma^*$ means that the considered buckling occurs simultaneously for both global stiffened plates and local plate panels. When the width-thickness ratio b_ℓ/t changes from 30 to 60, each ultimate strength for G1 and G2 is found to agree with that for L2 and L3, respectively, in $\sigma_{xm} < \sigma_{ym}$, and also the strength for G2 and G1 is found to agree with that for L2 and L5(or L4), respectively, in $\sigma_{xm} > \sigma_{ym}$. Therefore, for elastic buckling with larger width-thickness ratio, the ultimate strength for the global buckling tends to agree with that for the local buckl-

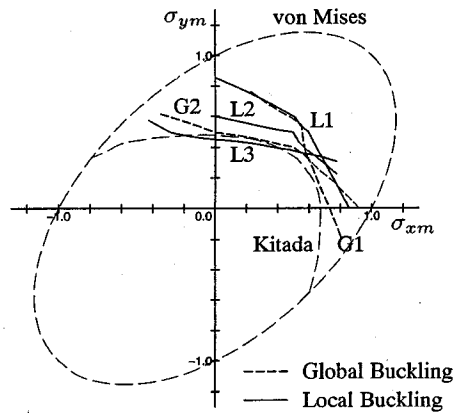

Fig. 8 Interaction curves for square stiffened plates ($b_\ell/t = 40, W_o t = b_\ell/150$).

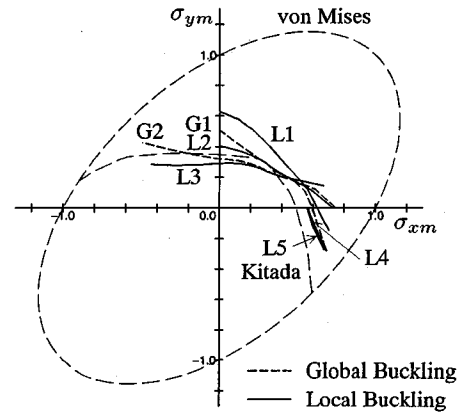

Fig. 9 Interaction curves for square stiffened plates ($b_\ell/t = 60, W_o t = b_\ell/150$).

ing. Of course, from **Fig. 2**, it is shown that, independent of the value of width-thickness ratio, the elastic buckling strength, *i.e.* the elastic buckling coefficient, for the global buckling coincides with that for the local buckling when $\gamma = \gamma^*$.

The present method does not take into account an effect of the interaction of several initial deflection modes on the ultimate strength. However, from above numerical demonstrations, it is found that this method can evaluate the ultimate strength for simultaneous bucklings of global stiffened plates and local plate panels with as proper accuracy as the Kitada's finite element results. In other words, the effect of the interaction of both global and local initial deflections on the strength by Kitada is considered as the effect of a global or local distinct initial deflection with the same level of the magnitude in this method.

4. CONCLUSIONS

The ultimate strength of rectangular steel stiffened plates under biaxial in-plane forces of tension and/or compression is predicted by this unified simple method. The main conclusions are:

(1) The present approach is formulated for general rectangular longitudinally stiffened plates, and is demonstrated as ultimate strength interaction curves for square stiffened plates with two longitudinal stiffeners.

(2) For given residual stresses and initial deflections, the elasto-plastic strength for the 'imperfect' stiffened plate may be explicitly predicted in the form of the unified imperfection sensitivity curve near the 'equivalent bifurcation point', at which the elasto-plastic post-buckling equilibrium path for the 'perfect' stiffened plate intersects its plastic failure mechanism curve.

(3) The actual initial deflection mode is modified and replaced by the 'equivalent initial deflection mode'.

(4) The present ultimate interaction curves are found to be in agreement with the Kitada's numerical results for intermediate practical ranges of width-thickness ratios.

(5) All the calculations herein can be executed readily using only a personal computer with small memory storage.

(6) The general philosophy adopted in this paper may also be applicable to other types of structures such as rigid frames, arches and trusses as well as columns, beam-columns, plates, cylindrical shells and cylindrical panels.

REFERENCES

1) Timoshenko,S.P. and Gere,J.M. : *Theory of Elastic Stability, Second Edition,*. McGraw-Hill, New York, 1961.

2) Allen,H.G. and Bulson,P.S. : *Background to Buckling.* McGraw-Hill, 1980.

3) Fukumoto,Y.(Ed.) : *Guidelines for Stability Design of Steel Structures.* JSCE, 1987.

4) Prabhakara,M.K. and Chia,C.Y. : Post-buckling behaviour of rectangular orthotropic plates. *J. Mech. Eng. Sci.*, Vol. 15, pp.25-33, 1973.

5) Libove,C. : Buckle pattern of biaxially compressed simply supported orthotropic rectangular plates. *J. Composite Materials*, Vol. 17, pp.45-48, 1983.

6) Haslach,Jr.,H.W. : Post-buckling stability of orthotropic, linear elastic, rectangular plates under biaxial loads. *Int. J. Mech. Sci.*, Vol. 28, pp.739-756, 1986.

7) Zhang,J.-W. and Shen,H.-S. : Postbuckling of orthotropic rectangular plates in biaxial compression. *J. Eng. Mech.*, ASCE, Vol. 117, pp.1158-1170, 1991.

8) Ueda,Y., Sherif,Rashed,M.H. and Paik,J.K. : Elastic buckling interaction equation of simply supported rectangular plates subjected to five load components. *J. Sci. Naval Architects of Japan*, No. 157, pp.425-438, 1985(in Japanese).

9) Valsgård,S. : Numerical design prediction of the capacity of plates in biaxial in-plane compression. *Computers & Structures*, Vol. 12, pp.729-739, 1980.

10) Dier,A.F. and Dowling,P.J. : The strength of plates subjected to biaxial forces. *Behaviour of Thin-Walled Structures* (Ed. by J.Rodhes and J.Spence), pp.329-353, Elsevier Applied Science Publishers, 1984.

11) Narayanan,R. and Shanmugam,N.E. : Compressive strength of biaxially loaded plates. *Plated Structures – stability and strength* (Ed. by R.Narayanan),pp.195-219, Applied Science Publishers, 1983.

12) Inoue,T., Komiya,N. and Kato,B. : Flexural rigidities and buckling of steel plates in the plastic flow range under biaxial stress. *Trans. Arch. Inst. of Japan*, No. 371, pp.1-13, 1987(in Japanese).

13) Ohtsubo,H. and Yoshida,Y. : Ultimate strength of rectangular plates under combination of loads (Part 1). *J. Sci. Naval Architects of Japan*, No. 156, pp.323-329, 1984(in Japanese).

14) Mikami,I., Kimura,T. and Tokuda,K. : An investigation on the ultimate strength of biaxially compressed single panel. *Proc. 46th Annual Conf. JSCE*, I-63, pp.164-165, 1991(in Japanese).

15) Kitada,T., Nakai,H., Furuta,T. and Suzuki,H. : Ultimate strength of stiffened plates subjected to biaxial in-plane forces. *J. Struct. Eng.*, Vol. 34A, pp.203-214, 1988(in Japanese).

16) Kitada,T., Nakai,H. and Furuta,T. : Ultimate strength and interaction curve of stiffened plates subjected to biaxial in-plane forces. *Struct. Eng./Earthq. Eng., Proc. JSCE*, Vol. 8, pp.113s-122s, 1991.

17) Kumagai,Y., Iura,M. and Yoshida,S. : A design approach of stiffened plates subjected to biaxial in-plane forces. *J. Struct. Eng.*, Vol. 39A, pp.143-152, 1993(in Japanese).

18) Isami,H. : A new strength prediction method for biaxially compressed plates. *Theo. Appl. Mech.*, Vol. 39, pp.109-118, 1990.

19) Isami,H. : A new approach to predict the strength of steel rectangular plates under biaxial in-plane compression. *J. Struct. Eng.*, Vol. 37A, pp.219-228, 1991(in Japanese).

20) Niwa,Y., Watanabe,E. and Isami,H. : A new approach to predict the strength of compressed steel stiffened plates. *Struct. Eng./Earthq. Eng., Proc. JSCE*, Vol. 2, pp. 281s-290s, 1985.

21) Isami,H. : A simple approach to predict the ultimate strength of biaxially compressed stiffened plates. *J. Struct. Eng.*, Vol. 38A, pp. 231-242, 1992(in Japanese).

22) Bleich,F. : *Buckling Strength of Metal Structures.* McGraw-Hill, 1952.

23) Isami,H. : A failure mechanism curve for compressed rectangular plates. *Bull. Kochi National College of Technology*, No.33, pp. 83-91, 1990(in Japanese).

(Received July 2, 1993)

2方向面内力を受ける補剛板の終局強度推定法

勇　秀憲

本論文は，著者がこれまで提案してきた弾塑性耐荷力の統一的簡易評価法を，縦補剛材を有する矩形補剛板の2方向面内終局強度の推定に適用するものである．与えられた2軸方向のひずみ比に対して，まず弾塑性座屈強度が材料の弾塑性挙動と2軸方向の断面の残留応力から決定される．そしてその終局強度は，弾塑性後座屈釣り合い曲線と塑性崩壊機構曲線の交点である等価分岐点近傍で，荷重極値となるように初期不整の敏感性曲線として直接的に評価される．本評価法の数値解析例と従来の弾塑性大変形有限要素法による結果と比較することによりにより，本法の有用性と妥当性を検討するものである．